# US Department of Energy, Office of Science
# Office of Biological and Environmental Research (BER)
# Environmental Remediation Science Division (ERSD, now CESD)
# FY10 Third Quarter Performance Measure

## INTRODUCTION

The third FY10 ERSD overall Performance Assessment Rating Tool (PART) measure for Pacific Northwest National Laboratory is to '*Provide a report that describes pre-modeling calculations of a planned reactive transport field experiment along with comparative results from the completed experiment'*. This milestone is focused on research being performed at the Hanford Integrated Field Research Challenge (IFRC) site, located in the 300 Area of Hanford Site in southeastern Washington State. The 1600 $m^2$ Hanford IFRC site contains 36 groundwater monitoring wells placed within the footprint of the historic South Process Pond where uranium fuels-fabrication wastes were discharged. A 2 $km^2$ U(VI) groundwater plume exists at this location that exceeds regulatory limits. Uranium concentrations in the plume show complex seasonal changes that have not been predictable with any model applied. DOE is trying to identify a suitable and effective remedial strategy for the site.

The Hanford IFRC is investigating fundamental interactions between hydrologic, geochemical, and microbiologic processes that control uranium behavior in the plume with an emphasis on mass transfer. Mass transfer is a critical process controlling the longevity of the U plume and its remediation, and involves the rate of U exchange between grain interiors and bathing fluids, and between waters in less permeable and more permeable sediment facies. This understanding is developed through comprehensive field characterization, injection experiments with non-reactive tracers and different uranium concentrations, monitoring experiments during periods of hydrologic transients and water table oscillations, and reactive transport modeling that incorporates physical and chemical heterogeneities. An important aspect of the research is the performance of manipulative experiments to investigate in-situ mass transfer rates and adsorption/desorption kinetics controlling U plume dynamics. These experiments require careful planning to account for the realities and complexities of site hydrology (e.g., groundwater travel times and directions) and the anticipated time scales of multiple kinetic processes.

In this report we describe the application of a reactive transport model to simulate a series of hypothetical uranium injection experiments at the Hanford IFRC site. The model includes kinetic adsorption/desorption controlled by surface complexation and mass transfer, and a heterogeneous hydraulic conductivity field parameterized through various hydraulic tests (EBF measurements, pump testing, and tracer experiments). The hydraulic conductivity model and the kinetic adsorption desorption model were described in the first and second reports in this series. The geochemical model parameters, as defined by fitting laboratory experimental results with intact sediment cores, pose important constraints on potential field experiments, and require careful consideration. Ten hypothetical scenarios were simulated, and the model was applied to select field data

from a preliminary U(VI) injection experiment performed in October 2009. The collective results are evaluated to identify the best injection strategy for an in-situ uranium field experiment in early FY 2011.

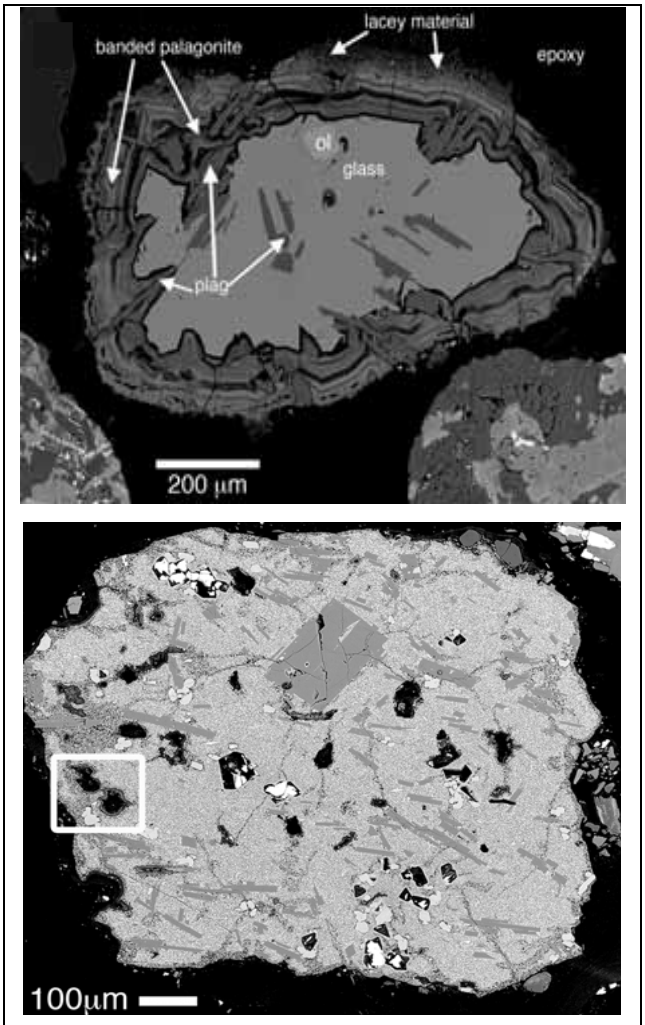


**Figure 1**. Uranium containing grains from 300A sediments displaying microporous weathering rinds and significant intergranular pore space .

## BACKGROUND

The Hanford IFRC is seeking to understand the field scale resupply and migration behavior of U within a persistent groundwater plume that has been in place for over 40 years. A number of laboratory studies using contaminated vadose zone and saturated zone sediments from the IFRC site have shown that U is adsorbed to the sediments by a surface complexation reaction (Bond et al., 2009). Additionally, it has been consistently observed that the adsorption-desorption process (forward and reverse surface complexation) is slow, displaying kinetic behavior over the time-scale of groundwater flow (Qafoku et al., 2005; Liu et al., 2008; and Liu et al., 2009). This kinetic behavior is believed to result from diffusive mass-transfer of U between adsorption sites of limited accessibility in grain coatings and intragrain pores and fractures (Figure 1; Stubbs et al., 2009). Characteristic of this behavior is: i.) slow leaching (desorption) of contaminant U from intact sediment cores with significant tailing (e.g., asymptotic approach to "zero concentration", and concentration rebound when advective flow is stopped (Figure 2a, b) and ii.) a long approach to full solute breakthrough during adsorption, and concentration rebound during stop flow after a pulse of U-spiked synthetic groundwater water migrates through an intact sediment column (Figure 2c).

Various model types have been evaluated for their ability to describe the noted laboratory-scale kinetic behavior of U in 300 A and IFRC sediments. The multi-rate model, described by Haggerty and Gorelick (1995), has been found to be the most effective through this evaluation. The governing equations for the multi-rate model were described in the second PART report. The model (Haggerty and Gorelick, 1998)

describes kinetic behavior as a consequence of a distribution of adsorption sites (50 in this case) that each exhibits a different first order rate constant (*k*) for adsorption-desorption that range from large/fast (at site 1) to small/slow (at site 50) (Figure 3a). All sites are assumed to exhibit the same adsorption affinity for U, as described by a constant $K_d$ at fixed pH and groundwater composition, or a common set of surface complexation parameters (log K and site concentration). These parameters were derived under conditions of fixed groundwater chemical composition by fitting the effluent U(VI) concentrations from three laboratory column experiments (only ICE-2 shown in Figure 2). The rate constants follow a log normal probability distribution with a mean of μ and a standard deviation of σ (Figure 3a). These rate constants yield different reaction half-lives for each site (Figure 3b).

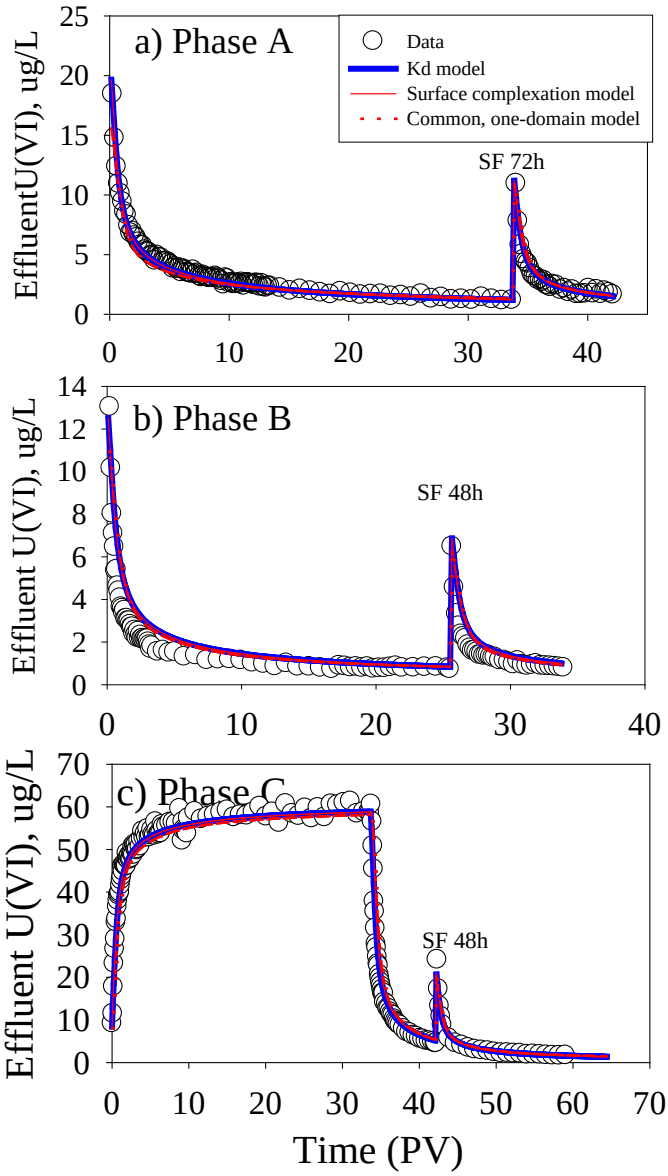


**Figure 2**. Measured and modeled breakthrough curves of U(VI) in desorption phase A (plot a), desorption phase B (plot b), and adsorption/desorption phase C (plot c) in column ICE-2.

The multi-rate model consequently supports the concept of reaction timescales (Haggerty et al., 2004), which is a critical consideration for a successful U injection experiment at the Hanford IFRC site. Sites with fast rate constants react to equilibrium quickly and participate in U adsorption-desorption reactions with rapidly moving injected waters of different composition. In contrast, the contact time for a migrating injected plume at the IFRC may be too short to allow appreciable reaction at sites with slow rate constants. Key is the relative distribution of rapidly and slowly reacting adsorption sites, and their reaction rates relative to groundwater flow. The 40 y persistence of the 300 A groundwater U plume has allowed the population of adsorption sites with very slow rate constants. Indeed, a large fraction of the adsorption sites in the IFRC sediments exhibit slow reaction rates.

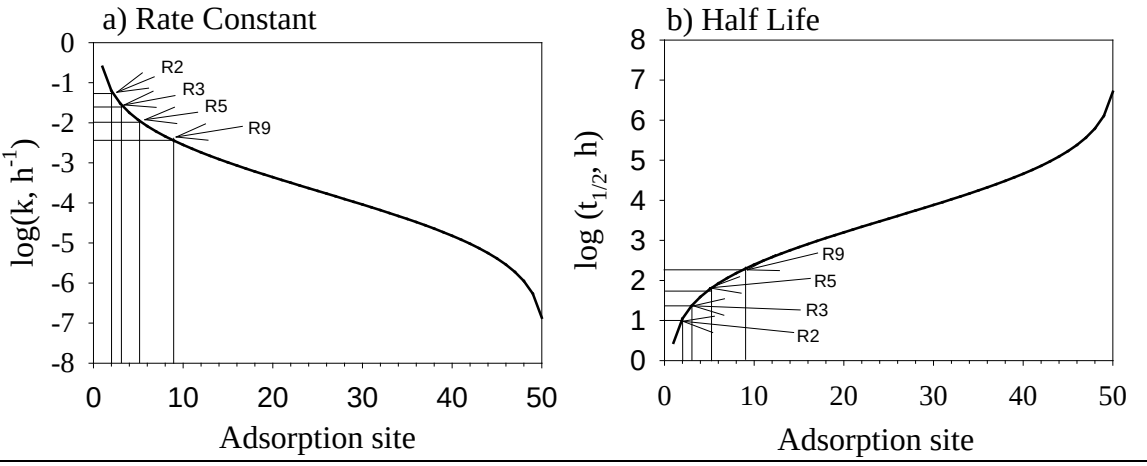


**Figure 3.** Multi-rate model site distributions, rate constants, and reaction half-lives. Sites 2, 3, 5, and 9 with rates R2, R3, R5, and R9 are discussed in the simulation results. The most aggressive injection scenarios (Cases 8, 9, and 10) accessed 5-10% of adsorbed U(VI) at site 25.

## REACTIVE TRANSPORT MODEL SIMULATIONS

### A. OBJECTIVES

The modeling goals were to identify injection volumes, rates, durations, and sequences that will enable field experimental evaluation of in-situ desorption/adsorption kinetics, as well as the applicability of the laboratory-derived reaction parameters. An experimental design is needed that will allow access to the largest number of adsorption sites that is possible given site hydrologic conditions. Desorption will be evaluated by injecting site groundwaters with background U concentrations (e.g., 5 µg/L) and possibly higher bicarbonate (e.g., 10 mM) than is present within the site [IFRC site groundwaters contain 35-90 µg/L U and 1.5 mM bicarbonate]. Adsorption experiments will utilize site groundwaters with higher U concentrations than are present at the site (e.g., 100-150 µg/L). Successful experimentation demands very specific in-situ time scales and concentration gradients given potential field scale reaction rates and known groundwater advective velocities.

### B. APPROACH and CONSTRAINTS

eSTOMP (the parallelized version of STOMP) and the multi-rate, surface complexation (MRSCM) uranium model described in the second PART report was used to simulate the reactive transport of U(VI) under a series of saturated zone U(VI) injection scenarios (Table 1). The simulations were performed on EMSL's Chinook supercomputer. The conditions for Case 2 were similar to an exploratory U injection experiment that was performed at the IFRC in October 2009. It is considered our base or reference case as its field behavior was relatively well documented. Initial simulations of this case were given in the second PART report. While the experiment was successful, it was complicated by unexpected river stage fluctuations during its performance. The

other scenarios evaluate the influence of injection rate (4, 5, and 10), injection duration (2, 6 and 7), pulsed injection (3 and 9), U concentration (1), and bicarbonate concentration (8).

Table 1. Injection scenarios (q1 = 681.4 liters per minute)

| Case Number | Injection Flow Rate | U Injection Concentration (µg/L) | Carbonate Injection Concentration (mM) | Injection Duration (hr) | Injection Strategy | Simulated Duration (hr) |
|---|---|---|---|---|---|---|
| Case 1 | q1 | 100 | 1.5 (Background) | 24 | Continuous | 100 |
| Case 2 | q1 | 5 | 1.5 | 24 | Continuous | 100 |
| Case 3 | q1 | 5 | 1.5 | 24 | Pulse (6 hr on, 6 hr off) | 100 |
| Case 4 | 5 q1 | 5 | 1.5 | 24 | Continuous | 100 |
| Case 5 | 0.5 q1 | 5 | 1.5 | 48 | Continuous | 100 |
| Case 6 | q1 | 5 | 1.5 | 48 | Continuous | 100 |
| Case 7 | q1 | 5 | 1.5 | 120 | Continuous | 300 |
| Case 8 | q1 | 5 | 10 (High) | 120 | Continuous | 300 |
| Case 9 | q1 | 5 | 1.5 | 120 | Pulse (12 hr, 24 hr off) | 516 |
| Case 10 | 0.25 q1 | 5 | 1.5 | 480 | Continuous | 660 |

The STOMP code uses modular approaches to solve multi-species reactive transport problems. Chemical reactions are solved in the reaction module and transport (advection and dispersion) is solved in the transport module. The modules are linked through an operator-splitting numerical scheme. All reactions including equilibrium and kinetic reactions are solved iteratively for each time step within the reaction module until convergence before supplying calculated results to the transport module in the code. For the multi-rate surface complexation reactions, however, this numerical implementation has caused a convergence problem in the reaction module because the rate constants in the multi-rate expressions range over 6 orders of magnitude (Figure 3). Consequently, solving the set of ordinary differential equations describing multi-rate adsorption kinetics requires a small time step for convergence. In the modified STOMP code, the multi-rate expressions have been moved out of the reaction module and the reaction module is used only to calculate equilibrium aqueous speciation. The calculated species concentrations are then used to calculate the equilibrium adsorption extent (Q) in the multi-rate expressions. Once Q is obtained, the first order multi-rate expressions are analytically solved. Unlike in the original STOMP code, there is no iteration between the multi-rate surface complexation reactions and aqueous speciation reactions in the modified code. The advantage of this approach is that it significantly improves computational efficiency. The disadvantage is that there may be computational errors that result from lack of iteration between the kinetic and equilibrium reactions. Numerical tests, however, found

that such errors are negligible for the U(VI) reactive transport in the column experiments. The modified code was used for simulating U(VI) reactive transport at the IFRC site.

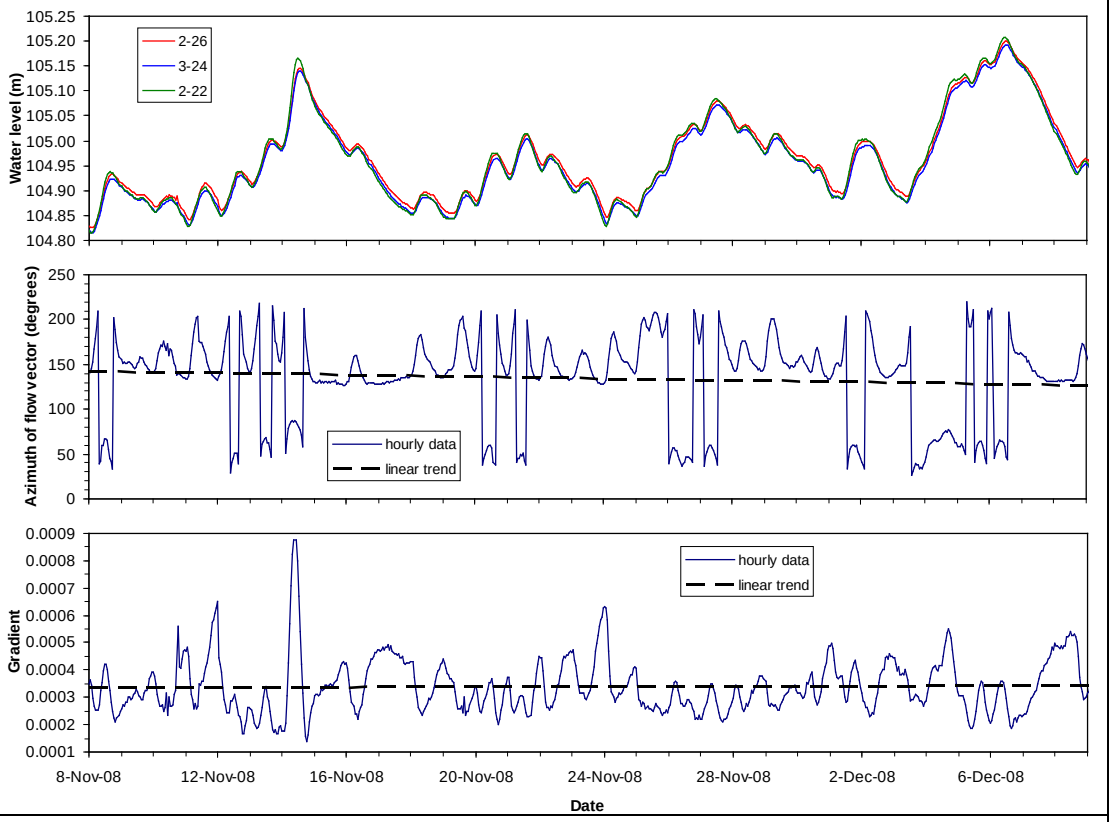


**Figure 4.** River stage (a.), azimuth or groundwater flow vector (b.), and gradient (c.) from November 2008.

The modified STOMP model contained a heterogeneous 3-D hydraulic conductivity model of the IFRC site as described in the first PART report. Uniform geochemical conditions were assumed for the simulations, as well as uniform porosity, particle density, mass fraction of < 2 mm sediment (the reactive fraction), and contaminant U distribution. The reactive fraction of the IFRC sediments (< 2 mm) is known through characterization to display marked heterogeneity across the site, with significant impacts expected on reactive transport. This heterogeneity was not considered in these initial simulations because of the complexity in doing so; it is, however, a future target. The initial adsorbed U concentration was established by equilibrating 35 µg/L U-groundwater with sediment throughout the entire simulation domain. Thus, the initial geochemical state was at surface complexation equilibrium. A groundwater U concentration of 35 µg/L was observed at the beginning of the field experiment in October 2009. The measured hydrologic conditions in the Columbia River during our November 2008 tracer experiment (Figure 4) were used to define groundwater directions and velocity. The injection start-time for all cases was 8-Nov-08 12:00 a.m.

C. RESULTS

C1. Case Studies

Well 2-9 was used for injection in all simulations (Figure 5). For tractable discussion we focus on Wells 2-9 and 2-14 only, and emphasize the results of Cases 5 and 8-10 (Figures 6-10) as being representative of different important behaviors. In concluding this discussion of results, we focus on the total loss of adsorbed U(VI) from the entire IFRC well field for Cases 2-10 (Figure 11). In the results that follow we describe the simulated concentrations of non-reactive tracer, $U(VI)_{aq}$, and adsorbed U(VI) at the chosen wells for the chosen scenarios. For adsorbed U(VI) we present concentration profiles for the primary sites that were computed to be reactive over the time frame of the injection and plume migration. Three general conclusions were found: i.) only a subset (20-30%) of the adsorption sites were reactive over the time frame of the simulated field experiments, ii.) a significant fraction of the adsorbed U(VI) inventory did not participate in the experiment because of slow reaction rates, and iii.) the overall degree of retardation of $U(VI)_{aq}$ was low because the sediment texture was coarse (e.g., 22% was < 2 mm and reactive), the overall adsorption site concentration of the sediment was low, and a small fraction of the available adsorption sites (0.2-0.3) were functional given the experiment time-scale.

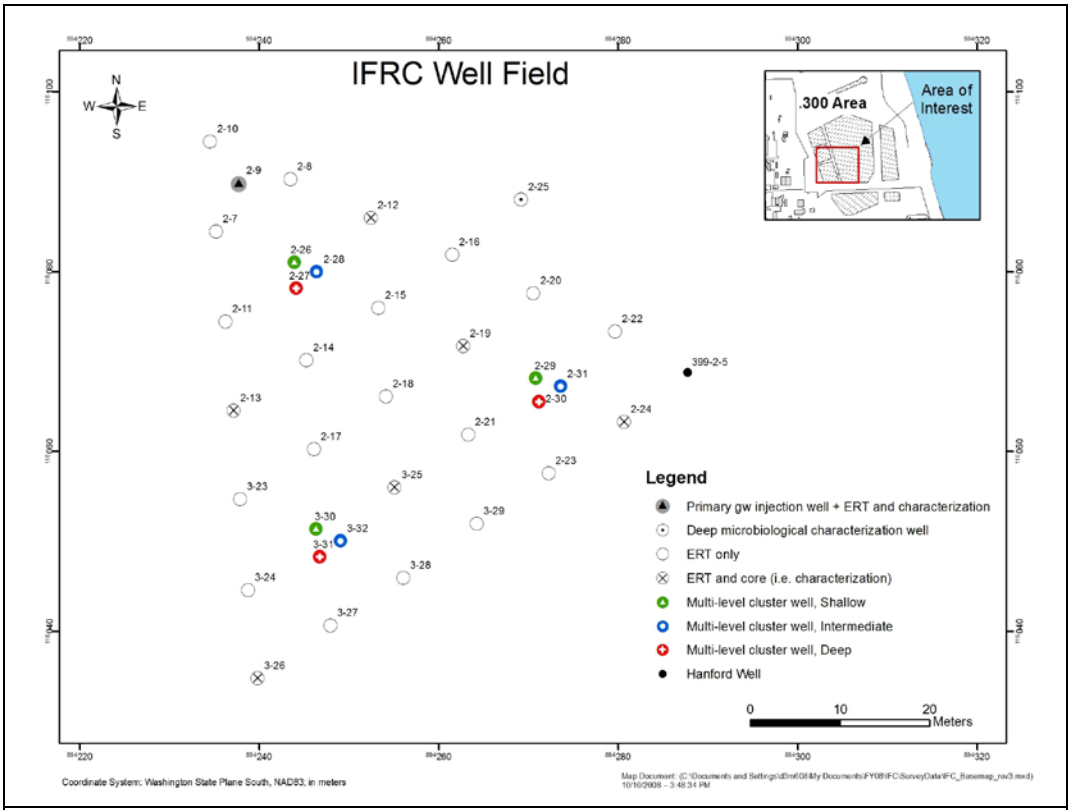


**Figure 5.** Plan view of the Hanford 300 Area IFRC well field. The predominant groundwater flow direction is southeast.

Case 5 involved a decrease in the injection rate (0.5q1) and an increase in injection duration (48 h, 2880 min) over our base case (Table 1); the total injection volume was the same (981,216 L). This injection sequence created a relatively narrow plume that advanced through and was totally contained within the IFRC well field (not shown, animations available on request). Tracer and 5 µg/L U(VI) dominated 2-9 well waters until injection ceased at ~3000 min (Figure 6a). During the course of injection, adsorbed U(VI) was removed beginning with the site with the most rapid rate constant (R2, see Figure 3). By the termination of injection, approximately 90% of U(VI) on R2 had desorbed. Sites R3, R5, and R9, each with progressively slower rate constants, followed this trend but each released proportionally less U(VI) because of their slower desorption rates. Site groundwaters (tracer = 0 and U(VI) = 35 µg/L) migrated into the well after injection and approximately 3000 min were required to return to background conditions. U(VI) was readsorbed/retarded during this period as shown by the increasing adsorbed U(VI) concentrations on all sites between 3000 and 6000 minutes. Tracer began to appear in downgradient Well 2-14, 21.5 m distant, after 1750 min (1.21 d) with 50% breakthrough occurring at 2800 min or 1.94 d (Figure 6c), yielding an average transport velocity of 11 m/d. Full breakthrough occurred after 5000 min (3.47 d). U(VI) breakthrough was similar to the tracer but desorption along the flow-path had increased concentrations in the plume core from 5 to 15 µg/L. This concentration increase caused significantly less desorption for the sediments surrounding Well 2-14 as compared to Well 2-9 (compare Figure 6b and 6d). Simulations of further down-gradient wells showed almost full dissipation of the low-U(VI) plume by the Well 3-25.

Case 8 was a long duration (7200 min, 120 h, 5 d) injection that created an initial plume of relatively large diameter that expanded beyond Wells 2-8 and 2-7 (not shown, animations available on request). The injected waters had a bicarbonate concentration (10 mM) that was 6.6 times the background concentration (1.5 mM). Bicarbonate enhances U(VI) desorption through formation of uranyl carbonate and calcium uranyl carbonate complexes that reduce the aqueous phase activity of the $UO_2^{2+}$ cation and its hydrolysis complexes. A dramatic river stage change at 9500 min caused a marked change in groundwater flow direction that influenced tracer and U concentrations in both reference wells (Figure 7). The injection of bicarbonate mobilized a small plume of U(VI) from the 2-9 well domain through enhanced desorption (Figure 7a). Significant U(VI) was removed from all reference adsorption sites (Figure 7b); sites 2 and 3 were cleaned off entirely. Adsorption recommenced on these sites after bicarbonate passage (after 16000 min) yielding aqueous U(VI) concentrations (26 µg/L) that were below background (35 µg/L). For this case 50% tracer breakthrough occurred at down-gradient Well 2-14 after 2300 min (Figure 7c) yielding a travel time of 13.5 m/d. A pulse of desorbed U(VI) (43 µg/L) is forecast to arrive immediately before the 0.5 tracer concentration. The impacts of down-gradient desorption within the plume are displayed by gradually increasing U(VI) aqueous concentrations with plume passage. The bicarbonate plume is very effective at down-gradient desorption, fully removing all adsorbed U(VI) from sites 1-5, and 65% of adsorbed U(VI) from site 9 (Figure 7d).

Case 9 was a sequential pulsed injection intended to create a low U(VI) concentration corridor down the center of the well field. The scenario consisted of 9 – 12 h (720 min)

injection periods followed by a 24 h (1440 min) rest stage, and then a final 12 h injection. Animations of tracer and U(VI) behavior during the course of the experiment reveal the effectiveness of this approach in developing a sustained zone of low U(VI) in the central region of the well-field (not shown, available on request). Because of relatively rapid groundwater movement at the site, the pulse injection scenario yielded a complex concentration trend for both tracer and U(VI) in injection Well 2-9 (Figure 8a). The "sawtooth trend" of increasing U(VI) with decreasing tracer during the injection phase (e.g., 0-20000 min) was a result of plume drift during the rest stages allowing inflow and mixing with background waters. The unequal changes in the heights of the concentration peaks associated with each injection-rest cycle were a result of river stage fluctuations that changed groundwater flow velocities during the course of the simulated experiment. The pulsed injection scenario was effective at the desorption of U(VI) from the injection well surroundings (Figure 8b), but complex behavior was noted for sites 2 and 3 that displayed oscillating adsorption and desorption events as a result of aqueous U(VI) concentration changes. The slow approach of $U(VI)_{aq}$ concentrations up to the background level (35 µg/L) after tracer departure is a result of the slow filling of rate-controlled adsorption sites (Figure 8b). The oscillatory concentration nature of the pulsed plume was moderated over the 21.5 m transport distance to Well 2-14 (Figure 8c), where a transport velocity of 11.5 m/d was observed for the plume. The concentration anomaly at 9800 min was a result of dramatic river stage change that temporarily changed plume position. Downgradient desorption was not as great as in the presence of bicarbonate (e.g., Case 8, Figure 7), yielding lower U(VI) plume concentrations and less sorbed U depletion in proximity to Well 2-14 (Figure 8c).

The final case discussed (Case 10) was similar in total injected volume to Case 9 (~ 5 million L), but the injected rate was slower and the duration longer. Animations of the simulation as compared to those for Case 9 (not shown, available on request) reveal that this approach was less effective in maintaining a stable region of low U in the center of the well field. The Case 10 plume was narrower, less stable with time, and more influenced by river stage changes and consequent groundwater trajectory changes. These effects were evident in Figure 9. The sustained, long duration injection was more effective in desorbing U(VI) from sediments surrounding Well 2-9 than was Case 9 (Figure 9b). In this case, sites 1-5 were desorbed to an equilibrium state with the injected water, while site 9 reached the lowest concentration of any treatment. Down-gradient tracer arrival was somewhat delayed (3200 min) relative to other cases, yielding an average travel time of 9.68 m/d (Figure 9c). Both tracer and U(VI) concentrations showed significant variability during plume passage (3200-35000 min) as a result of river stage variations and lateral plume movement. The extent of sorbed U depletion near Well 2-14 ranged from 20 to 50% from site 2 to 9. These were comparable to Case 9, but less than Case 8.

C2. Case Comparisons

There are a number of criteria that need be considered in planning a successful field desorption experiment that will be discussed in the next and final section, but by far the most important is to maximize the extent of desorption and the number of sites

participating in the experiment. These two factors go hand-in-hand because as desorption depletes adsorbed U(VI) on one site class, another begins to become accessible. Consequently another way to evaluate the different scenarios is to consider cumulative adsorbed U(VI) loss in sediments proximate to reference wells 2-9 and 2-14 (Figure 10). The scenarios were divided into two groupings to facilitate discussion: those with injection duration ranging from 24-48 h (Cases 2-6) and those with injection duration $\geq$ 120 h (Cases 7-10).

Cumulative U(VI) loss from injection Well 2-9 was similar for all short duration cases over the first 2500 min of injection, after which differences became apparent (Figure 10a). Case 2, representing similar conditions to our October 2009 exploratory experiment was least effective in mobilizing U from the injection well. Case 6, simply representing a doubling of injection duration (to 48 h) and volume (to 2 million L) over Case 2 was the most effective, mobilizing 0.009 g. All longer duration injections mobilized larger amounts of adsorbed U(VI) from Well 2-9 (Figure 10b). All cases followed similar trajectories at short time (e.g. 0-200 h), but Case 8 (high bicarbonate) had the highest slope indicating the greatest mobilization potential. The slow continuous injection of Case 10 mobilized the most adsorbed U(VI) from the injection well (0.021 g). Bicarbonate concentration and injection duration are important factors determining the extent of U(VI) loss at the injection well.

The cumulative displacement of U(VI) from down-gradient Well 2-14 revealed significant differences from the injection well (Figures 10c and 10d). U(VI) desorption was less for all cases at the down-gradient well except for Case 8 with high bicarbonate. For the short duration injections, Case 4 with high injection rate (3407 liters per minute) and volume (~ 5 million L) was by far the most effective, while reference Case 2 was least effective. [It should be noted that the conditions for Case 4 are unlikely to be achieved with our current site infrastructure. The scenario was included to demonstrate the impacts of high, short term injection rate and volume.] For the longer duration scenarios, Case 8 with high bicarbonate mobilized the most U(VI), followed by the long duration pulsed (Case 9) and continuous (Case 10) injection. Two particular comparisons deserve note. Cases 4 and 7 injected the same volume but with a 5-fold difference in injection rate, and longer duration. Case 7 desorbed close to 30% more U(VI) than case 4 (Well 2-14). Cases 7 and 9 injected the same volume, but Case 9 utilized a pulsed delivery that promoted 25% more desorption than Case 7. Consequently, duration, volume, and bicarbonate promote desorption in the down-gradient well.

A final quantitative metric worth considering for the various scenarios is cumulative loss of adsorbed U(VI) from the entire IFRC domain (Figure 11). This metric is strongly dependent on the areal extent of the plume footprint. With all other conditions being equal, a larger plume will contact more wells and sediment, and will mobilize more U. Animation results for Cases 8, 9, and 10 (not shown) provide a qualitative sense for plume footprint with areal extent decreasing in the following sequence: Case 8 > Case 9 > Case 10. Areal extent for all cases followed the series: Case 4 > Cases 7 and Case 8 > Case 9 > Case 6 > Case 10 > Cases 2, 3, and 5. Case 4 with high areal extent and high down-gradient desorption (Figure 10c) promoted the largest removal of U from the IFRC domain (160 g) for all short duration scenarios (Figure 11a). Case 8 with high areal

extent, high bicarbonate, and high down-gradient desorption (Figure 10d) was the most effective of all treatments mobilizing over 1 kg of adsorbed U(VI) from the IFRC domain (Figure 11b).

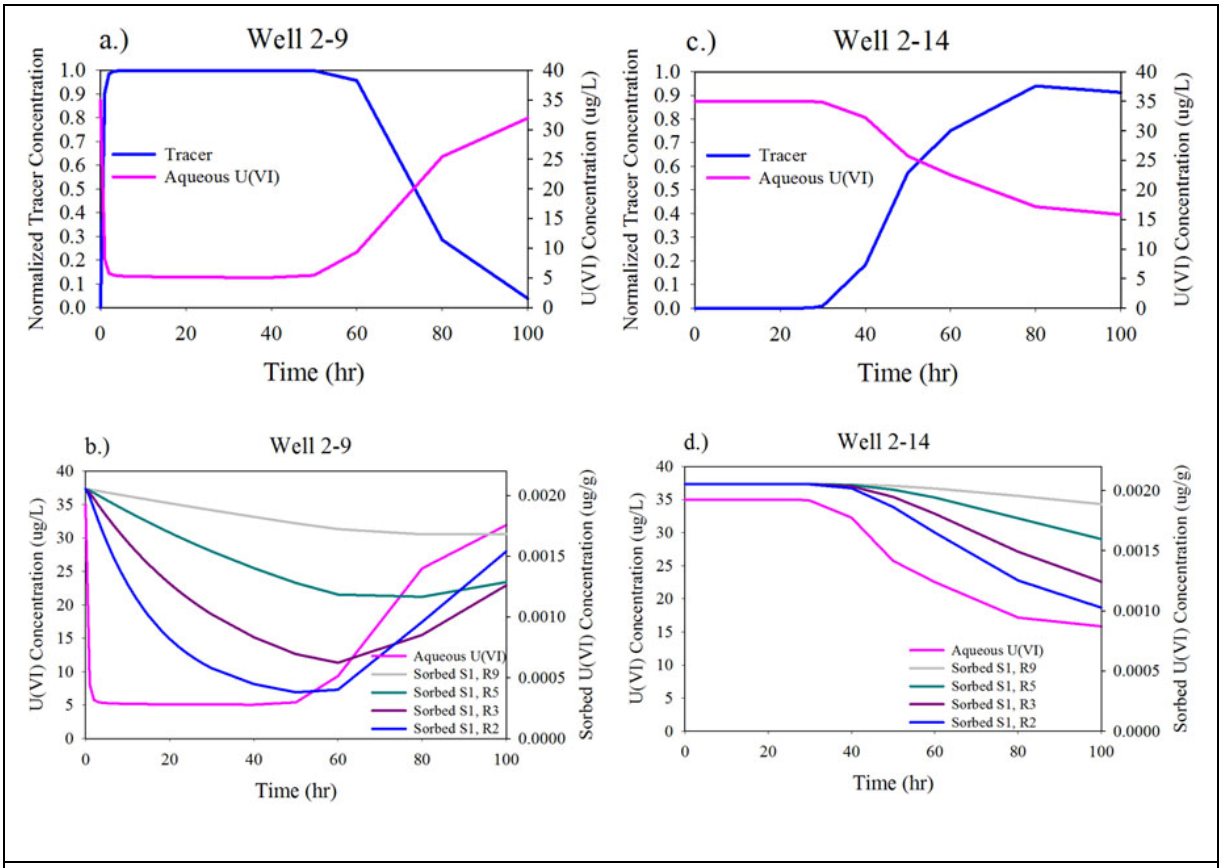


**Figure 6**. Simulation results for Case 5, Wells 2-9 and 2-14; a.) and b.) normalized tracer and $U(VI)_{aq}$; c.) and d.) adsorbed U(VI) for sites #2, 3, 5, and 9.

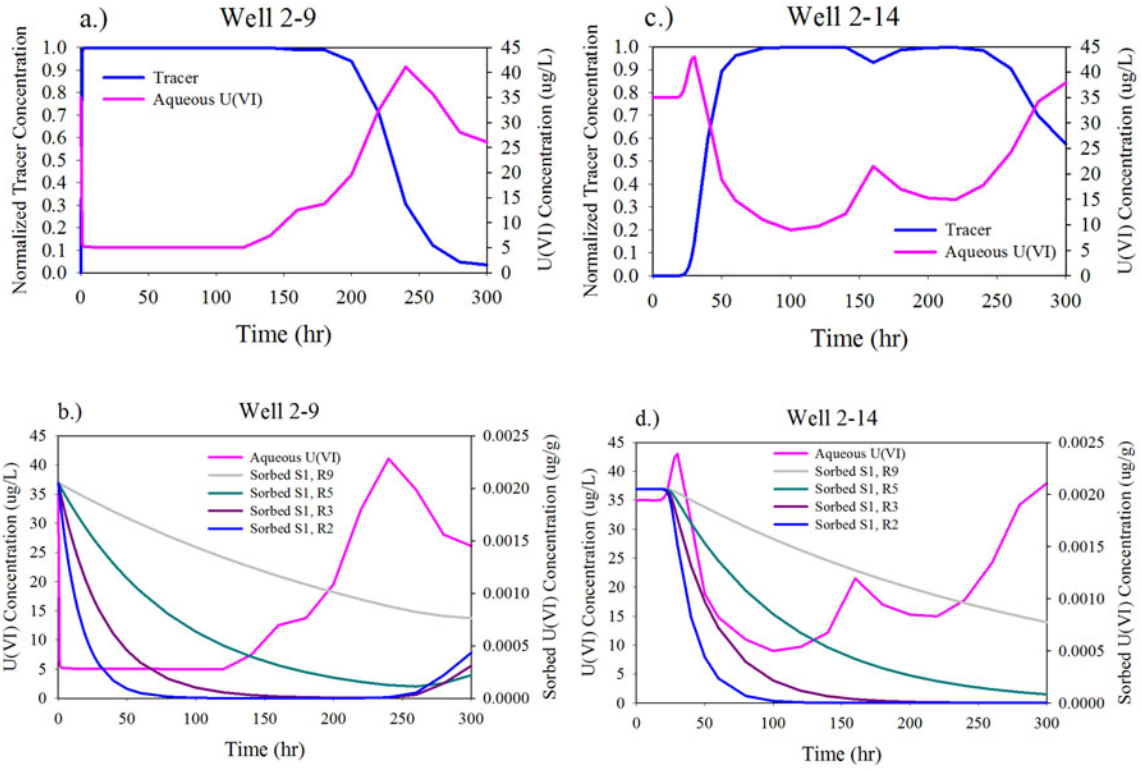


**Figure 7.** Simulation results for Case 8, Wells 2-9 and 2-14; a.) and b.) normalized tracer and $U(VI)_{aq}$; c.) and d.) adsorbed U(VI) for sites #2, 3, 5, and 9.

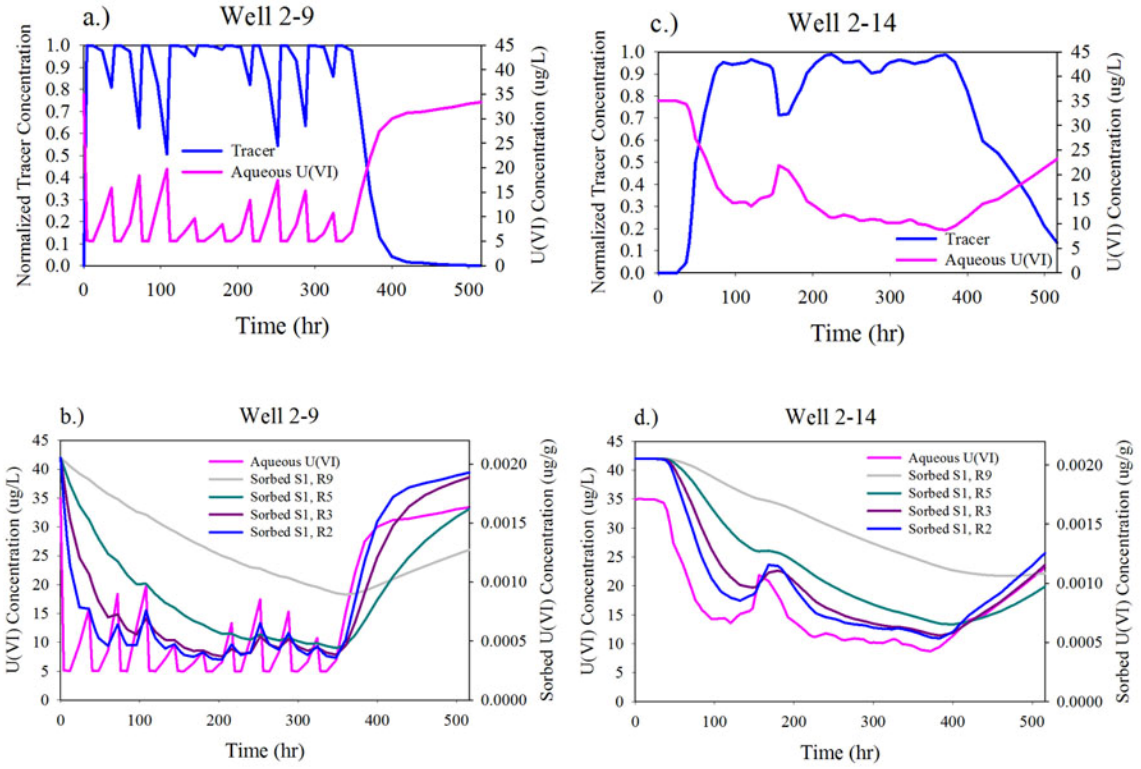


**Figure 8.** Simulation results for Case 9, Wells 2-9 and 2-14; a.) and b.) normalized tracer and $U(VI)_{aq}$; c.) and d.) adsorbed U(VI) for sites #2, 3, 5, and 9.

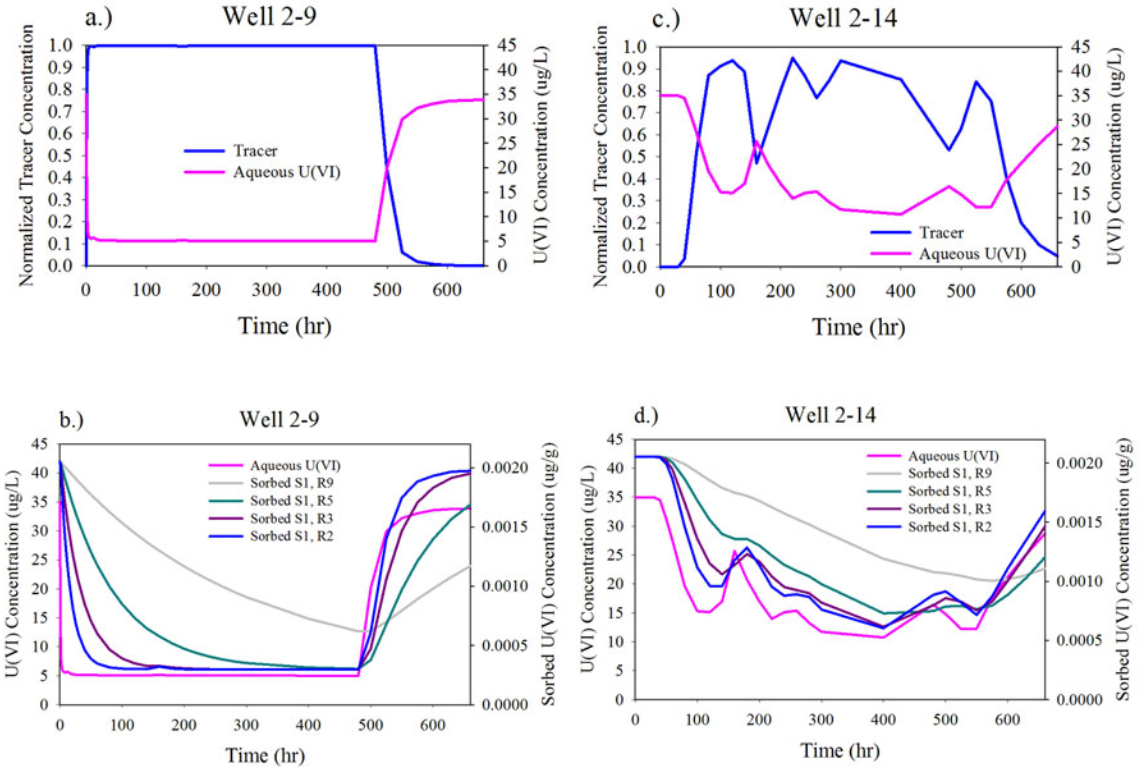


**Figure 9.** Simulation results for Case 10, Wells 2-9 and 2-14; a.) and b.) normalized tracer and $U(VI)_{aq}$; c.) and d.) adsorbed U(VI) for sites #2, 3, 5, and 9.

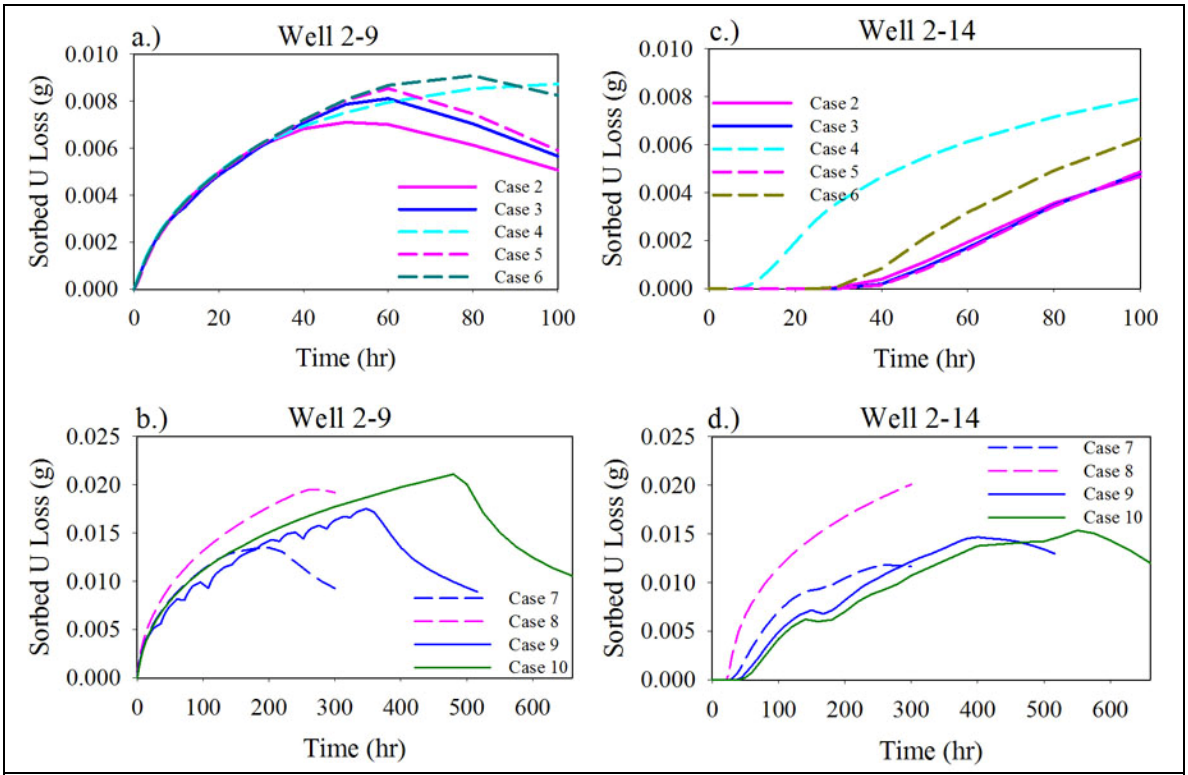


**Figure 10.** Total loss of adsorbed U(VI) from Wells 2-9 and 2-14 for all scenarios a.) and b.) Cases 2-6; c.) and d.) Cases 7-10.

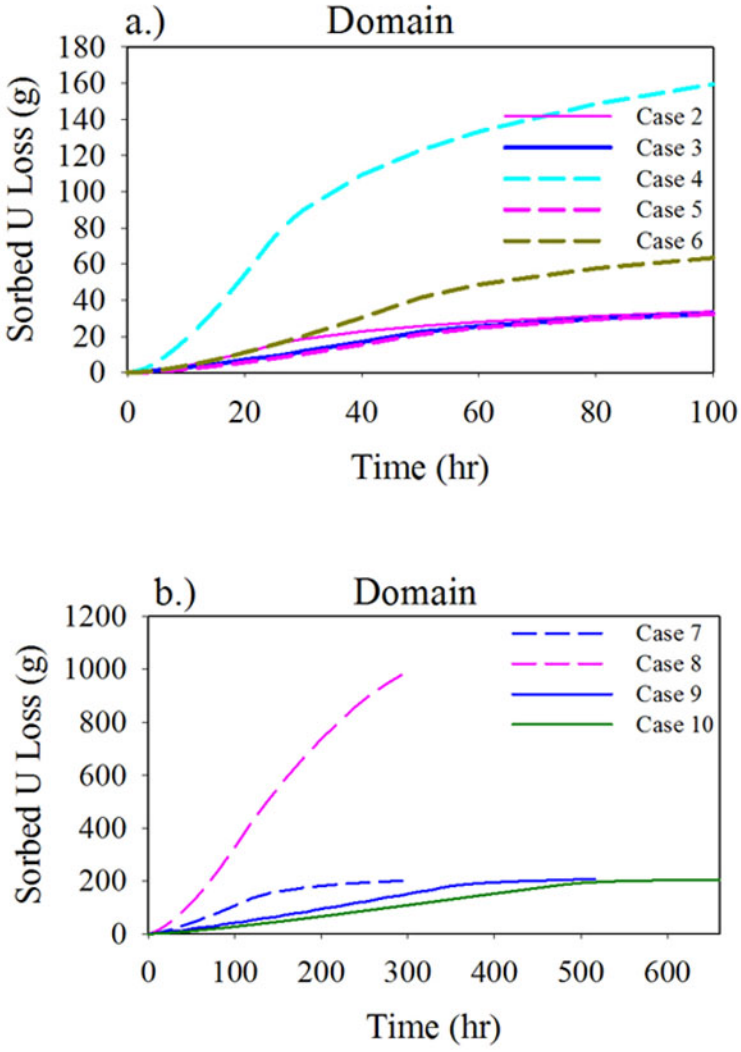


**Figure 11.** Total loss of adsorbed U(VI) from the IFRC domain for all scenarios a.) and b.) Cases 2-6; c.) and d.) Cases 7-10.

## COMPARISONS WITH FIELD DATA

An exploratory U(VI) injection experiment was performed in October 2009 to test site infrastructure, and to obtain preliminary data on the response of U(VI) to perturbations in groundwater composition for more robust experimental planning. The experiment was performed during a period of projected stable river conditions, and before the project had the capability to pre-model potential experiment behavior as performed in this report. Thus, the field experimental conditions were not optimized.

The experiment was similar to Case 2, and involved the injection of upgradient groundwater with 5 µg/L U(VI) and 180 mg/L bromide into Well 2-9 where the in-situ U(VI) concentration was 35 µg/L. The injection rate was q1 (Table 1) for 6.3 h (as compared to 24 h in Case 2), yielding an injected volume of 264,979 L. This lower injection volume was used to minimize the overall number of samples for U(VI) analysis (these are costly and the experiment was not expected to be a final one). Wells in the IFRC site were monitored for approximately 366 h while the plume (tracer) was within the domain of the well-field. However river stage oscillations began at 142 h that caused vertical flows in the wells that significantly influenced U(VI) results. An important finding overall was that the desorption plume dissipated earlier than we had expected. U(VI) concentrations within the plume returned to background concentrations (e.g., 35 µg/L) by the fourth well tier (e.g., 3-23, 2-17, 2-18, 2-19, and 2-20; Figure 5) through desorption. The calculations in this report were motivated by the desire to identify combinations of injection rate and duration that would propagate a desorption plume with at least 50% concentration reduction (e.g. to ~ 10-15 µg/L) of the native groundwater (35 µg/L) through all wells in the central core of the well-field.

The field experimental data from approximately eight individual wells was of sufficient quality to allow comparisons to simulations made with the model described in this report, and one of these is provided as an example (Figure 12). It is important to note that the hydrologic conditions during the October 2009 experiment were different from those used in the simulations in this report, and in Figure 12. However, the conditions were not so different during the early stages of the experiment (e.g., 0-100 h) allowing valid comparisons to be made between field experimental results from October 2009, and model calculations performed using November 2008 hydrologic data (e.g., those in Figure 4).

Generally, the model simulations for Well 2-9 were quite close to the experimental data (Figure 12) except for the injection phase (< 0 h). The injection phase, that involved the pumping of up-gradient groundwater from over 1 km distant, presented some operational details that were difficult to simulate. However, the observed and simulated behaviors were remarkably similar for the more important drift phase that began at 0 h. Close to 20 h were required for the plume to begin movement out of the well domain as indicated by the tracer behavior (e.g., normalized tracer = 1). Over this time period U(VI) increased in plume waters from 5 to 20 µg/L by release from the surrounding sediment through rate controlled desorption. The plume was slowly displaced from the well domain between 20 and 80 h as indicated by the tracer behavior. Deviations

between the observed and simulated tracer behaviors at 40-45 and 62-68 h were believed to result from well bore flows that allowed tracer-depleted waters into the sample domain. The simulated U(VI) concentration trend during this same period of plume displacement was similar to, but higher than that of observation; indicating that there was more retardation of returning U(VI) in the field as compared to that projected by the laboratory-based model. Overall, however, the model matched the field data from Well 2-9 very well indicating that the laboratory derived geochemical reaction parameters from intact sediment cores were field-relevant.

Other model simulations of the experimental data from the remaining seven wells ranged from very good to poor. We attribute these variable results to the effects of both physical and chemical heterogeneity. The physical heterogeneity model used in these calculations was an early one based on hydrologic measurements alone. That model has now been improved by incorporation of other measurement forms, including tracer breakthrough data from our highly successful March 2009 tracer experiment. The model used herein also assumed a homogeneous domain of: i.) adsorbed and groundwater U(VI) concentrations, ii.) adsorption site concentrations, and iii.) kinetic and surface complexation parameters. In contrast, characterization data from the site shows significant heterogeneity in these properties and parameters across the site. Future improvements to the model applied herein will, by necessity, need to consider geochemical heterogeneity.

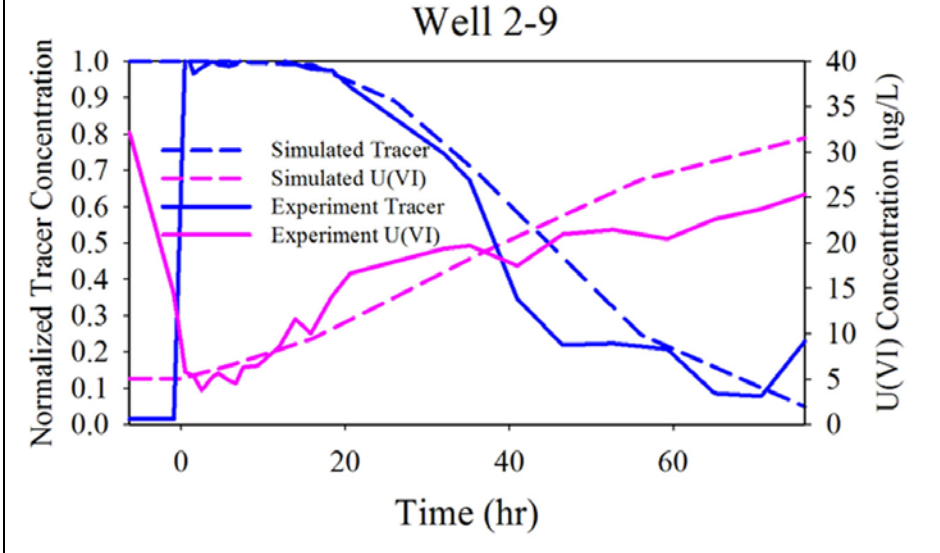


**Figure 12**. Model simulation and field results from October 2009 exploratory U desorption experiment for Well 2-9.

## IMPLICATIONS FOR FUTURE TRANSPORT EXPERIMENTS

The simulations described herein represent our first attempt to integrate a field-relevant kinetic model of U adsorption-desorption with the complexities of Hanford IFRC site hydrology. Laboratory experiments with intact IFRC cores revealed that a significant fraction of adsorbed contaminant U responds slowly to changes in aqueous chemical conditions as a result of intra-grain residence. This behavior was well described with a multi-rate surface complexation model containing an assemblage of adsorption sites displaying a large range in adsorption-desorption rate constants. Because groundwater flow velocities are high at the IFRC site (e.g., ~ 11 m/d) and trajectories change in response to river flow; integrative calculations of type performed here are essential to identify tractable operational and design conditions that will yield a successful field experiment. The primary goal of these simulations was to determine the type of plume that would maximize U desorption along the flowpath to allow robust evaluation of: i.) the kinetic geochemical reaction model developed under laboratory conditions and ii.) field scale features and phenomena influencing apparent kinetic behavior. The simulations were not intended to yield a final experimental design but rather to explore the complexity of the linked geochemical and hydrologic system and to identify the factors conducive to a successful experiment. More focused model calculations will now be performed on several select scenarios to address detailed questions of experimental design.

One important conclusion of the simulations was that the time frame for desorption is considerably longer than the average residence time of groundwater. Consequently, only a subset of adsorption sites accessed in the laboratory participated in the simulated field experiments. We provided metrics for sites 2-9 which represented approximately 25% of the total site concentration parameterized in lab experiments. Our most effective experiment (Case 8) was successful in desorbing over 65% of adsorbed U from site 9. Cases 8, 9, and 10 all induced significant desorption out to site 25-26 (Figure 3). This degree of desorption is not unexpected for the field because the higher degree of control afforded in laboratory experimentation allowed us to perform long-term experiments that accessed adsorption-desorption sites with extended half-lives (sites > 25). The time-scale necessary to investigate these slow sites is not necessarily accessible to us in the field without hydrologic control. The slow sites have become occupied during the long history of the plume; they do not appear active in seasonal U concentration changes observed within the saturated zone. Ongoing modeling activities are investigating whether hydrologic control by a dipole array is feasible for the IFRC site.

Optimal field experiment conditions can be identified under the constraint of keeping the injected plume within the IFRC well field to the maximum extent possible. This constraint is for the purpose of mass balance, moment analysis, and modeling. Given this constraint, it was evident from the various scenarios that injection volume, injection duration, and bicarbonate concentration were the primary factors that can be manipulated to maximize desorption extent. Cases 8, 9, and 10 accessed the largest range of adsorption sites and were demonstrative of these effects. Cases 9 and 10 were most effective in keeping the plume within the well field, and in creating an extended time

frame for desorption in the largest number of wells. It is recommended that further modeling attention be given to optimizing the pulsed and continuous injection approaches represented by Cases 9 and 10. The rest time between injected pulses in Case 9 and the injection rate in Case 10 are parameters that should be further varied to optimize plume stability/trajectory and in-site residence time. Moreover, the spiking of Na-bicarbonate into injected waters at a factor of 5-10 times the background concentration should be considered as an important component to any successful experiment. Additional geochemical calculations are currently ongoing to assess the range in elevated bicarbonate concentrations that can be injected into IFRC site groundwaters without inducing calcite precipitation.

References

Bond, D. L., J. A. Davis, and J. M. Zachara. 2008. Uranium(VI) release from contaminated vadose zone sediments: Estimation of potential contributions from dissolution and desorption, Chapter 14 in *Adsorption of Metals by Geomedia II: Variables, Mechanisms, and Model Applications*, (Ed. M. O. Barnett and D. B. Kent, pp. 375-416, Elsevier, Amsterdam, The Netherlands.

Haggerty, R. and S. M. Gorelick. 1995. Multiple-rate mass transfer for modeling diffusion and surface reactions in media with pore-scale heterogeneity. *Water Resour. Res.*, 31(10):2383-2400.

Haggerty, R. and S. M. Gorelick. 1998. Modeling mass transfer processes in soil columns with pore-scale heterogeneity. *Soil Sci. Soc. Am. J.*, 62(1), 62-74.

Haggerty, R., C. F. Harvey, C. F. von Schwerin, and L. C. Meigs. 2004. What controls the apparent timescale of solute mass transfer in aquifers and soils? A comparison of experimental results. *Water Resour. Res.*, 40, W01510.

Liu, C., J. M. Zachara, N. Qafoku, and Z. Wang. 2008. Scale-dependent desorption of uranium from contaminated subsurface sediments. *Water Resour. Res*., 44:W08413, doi:10.1029/2007WR006478.

Liu, C., Z. Shi, and J. M. Zachara. 2009. Kinetics of uranium(VI) desorption from contaminated sediments: Effects of geochemical conditions and model evaluation. *Environ. Sci. Technol.*, 43:6560-6566.

Qafoku, N. P., J. M. Zachara, C. Liu, P. L. Gassman, O. S. Qafoku, and S. C. Smith. 2005. Kinetic desorption and sorption of U(VI) during reactive transport in a contaminated Hanford sediment. *Environ. Sci. Technol.*, 39:3157-3165.

Stubbs, J. E., L. A. Veblen, D. C. Elbert, J. M. Zachara, J. A. Davis, and D. R. Veblen. 2009. Newly recognized hosts for uranium in the Hanford site vadose zone. *Geochim. Cosmochim. Acta,* 73:1563-1576.